Advanced Robotics

ISSN: 0169-1864 (Print) 1568-5535 (Online) Journal homepage: https://www.tandfonline.com/loi/tadr20

Decentralized controllers for perimeter surveillance with teams of aerial robots

Luciano C.A. Pimenta , Guilherme A.S. Pereira , Mateus M. Gonçalves , Nathan Michael , Matthew Turpin & Vijay Kumar

To cite this article: Luciano C.A. Pimenta , Guilherme A.S. Pereira , Mateus M. Gonçalves , Nathan Michael , Matthew Turpin & Vijay Kumar (2013) Decentralized controllers for perimeter surveillance with teams of aerial robots, Advanced Robotics, 27:9, 697-709, DOI: 10.1080/01691864.2013.778942

To link to this article: https://doi.org/10.1080/01691864.2013.778942

Advanced Robotics, 2013
Vol. 27, No. 9, 697–709, http://dx.doi.org/10.1080/01691864.2013.778942

Taylor & Francis
Taylor & Francis Group

FULL PAPER

Decentralized controllers for perimeter surveillance with teams of aerial robots

Luciano C.A. Pimenta[a], Guilherme A.S. Pereira[a]*, Mateus M. Gonçalves[a], Nathan Michael[b], Matthew Turpin[c] and Vijay Kumar[c]

[a]*Escola de Engenharia, Universidade Federal de Minas Gerais, Belo Horizonte, MG 31270-901, Brazil;* [b]*Robotics Institute, Carnegie Mellon University, Pittsburgh, PA 15213, USA;* [c]*Department of Mechanical Engineering and Applied Mechanics, University of Pennsylvania, Philadelphia, PA 19104, USA*

(*Received 3 September 2012; accepted 21 December 2012*)

This paper presents a decentralized controller to guide a group of aerial robots to converge to and to move along a simple closed curve specified in a three-dimensional environment. This curve may be considered as a perimeter to be surveilled by the robots. The solution presented in this paper is based on an artificial vector field modulated by a collision avoidance scheme and relies only on local sensing. Proofs of asymptotic stability of the proposed controller are devised for a team of kinematically controlled rotorcrafts. Experimental results with a group of autonomous quadrotors are presented to validate the applicability and performance of the approach.

Keywords: aerial robots; swarms; vector fields

1. Introduction

Aerial robots are particularly adept to the application of surveillance due to their maneuverability and extended workspace in comparison to ground robots. However, there are several challenges in developing a viable surveillance approach. In particular, we must ensure that the robots maintain some continuous coverage of the environment. Further, as we wish to pursue methods that leverage large numbers of robots to cover large spaces, the planning and control problems must guarantee convergence, regardless of the system size. In this work, we focus on an approach that relies on decentralized individual robot control laws that drive a team of aerial robots to converge to and circulate along a curve in a three-dimensional environment.

Several research groups have addressed the problem of controlling one or more mobile robots to converge to (and sometimes circulate along) a desired one dimensional curve,[1–7] enabling tasks such as perimeter surveillance and boundary coverage,[8] environmental monitoring,[9] tracking of mobile targets [10] and artistic pattern formation.[11]

Although convergence of teams of mobile robots to curves is not a recent problem (e.g. the work of Sugihara and Suzuki [12]), most solutions found in the literature address two-dimensional environments. This is the case, for example, of the work by Hsieh et al. [8], where the authors present provably correct and decentralized solutions to control large groups of planar mobile robots to converge to closed curves. A few authors have proposed methodologies that control mobile robots in three-dimensional workspaces. In [5], the authors propose a 3D vector field to guide a single aerial mobile robot to converge to planar curves. The authors of [2] suggest a similar methodology but consider generic, time-varying curves.

The focus of this paper is the development of a control solution for a large team of micro-aerial vehicles (MAVs) to converge to and circulate along a closed curve in a three-dimensional workspace while avoiding inter-robot collisions. As we aim to work with groups of tens or hundreds of robots (i.e. swarms), we pursue a strategy that relies only on local sensing and limited inter-robot communication.

The methodology proposed in this paper is based on vector fields, which are extensively used to control aerial robots.[3,13–16] An advantage of vector field-based techniques over traditional methods is the fact that it is often possible to specify a potential function, whose gradients determine the field, and use such a function as a Lyapunov function to formally show the system stability.[10] Another advantage is that vector fields may be locally modified without compromising the global properties of the system.[17] This property is very important in multi-

*Corresponding author. Email: gpereira@cpdee.ufmg.br

robot scenarios where we are dealing with dynamic constraints imposed by other robots in the group.

The solution that we propose in this paper builds upon our earlier work,[2] where the vector field is composed of two terms: (i) a gradient term that attracts the robots to the target curve and (ii) a tangential term that is orthogonal to the first one that drives the robots to circulate along the curve. These two components are based on two implicit functions (n–1 functions for n-dimensional spaces), which also define the target curve. A practical methodology to specify the implicit functions based on a set of sample points of the target curve is also presented in [2].

Differently from [2], which was designed to control a single robot, in the present work, to allow robot cooperation, the field has three components: two components with negative projection onto the gradient term and a tangential component, orthogonal to the other two. To avoid collisions among the robots (which are considered to be spherical), each term of the field is modulated based on a set of priority values computed online based on local information acquired from neighboring robots. This scheme is similar to the 2D version proposed in [18], where a single potential function is used to specify the target curve. In [18], the evaluation of this function at each robot's configuration along with the robot's instantaneous velocity imposed by the vector field is used to compute the priority of the robot among its neighbors. Priorities are defined at the orthogonal and tangential directions to the curve, forcing the robots to slow-down or speed-up in each of these component directions to avoid collisions. Since in the present paper we are considering a 3D workspace, the prioritization scheme of [18] cannot be directly used. Thus, we define priorities in three directions: two directions related to convergence to the curve, and one direction orthogonal to the other two, which is tangent to the curve. With this methodology, we are able to guarantee that a group of kinematically controlled, spherical holonomic robots converge to and circulate along curves in 3D. Our proofs are valid for a large class of curves, for which we present conditions that may be verified before the execution of the task.

To the authors' best knowledge, the methodology presented in this paper is the first provably correct decentralized solution that controls a group of mobile robots to converge to and circulate along curves specified in three dimensions. Furthermore, the robots may be heterogeneous in physical size and sensing. Another important contribution of the paper is the experimental validation of the methodology with a team of indoor quadrotor robots.

The next section formally presents the problem statement and Section 3 details the proposed methodology to solve the problem. Formal proofs of convergence of such a methodology are presented in Section 4. Experimental results with aerial robots are discussed in Section 5. Finally, Section 6 presents conclusions and provides possible future research directions.

2. Problem statement

Consider a set Ω of N spherical robots, such that to a given robot ω_i is associated a radius r_i and a spherical sensing range with radius R_i. For every instant of time $t \geq 0$, we define the configuration $\mathbf{q} = [x(t)\, y(t)\, z(t)]^T \in \mathbb{R}^3$, where x, y, and z denote Cartesian coordinates, and assign to each robot a unique configuration $\mathbf{q}_i(t)$ corresponding to the position of the sphere center. The model for all robots $\omega_i \in \Omega$ is holonomic and purely kinematic:

$$\dot{\mathbf{q}}_i = \mathbf{u}_i, \tag{1}$$

where $\dot{\mathbf{q}}_i$ is the velocity vector of robot i and $\mathbf{u}_i$ is its control input.

Let $\alpha_i(x,y,z): \mathbb{R}^3 \mapsto \mathbb{R},\ i \in \{1,2\}$ be functions with continuous partial derivatives. Function α_1 depends only on x and y. Also, the projections of any level surface of α_1 onto a plane parallel to the plane xy must be a Jordan curve (e.g. closed, continuous, and all its parameterizations are injective maps). Notice, that any level surface of this function, $\alpha_1(\mathbf{q}) = C$, where C is a constant, is cylindric.

Function α_2 is of the form

$$\alpha_2(x,y,z) = \sigma z - \Phi(x,y),\ \sigma \neq 0 \tag{2}$$

where $\Phi(x,y)$ is a function with continuous partial derivatives. It can be seen that the level surfaces of α_2 do not have two points with the same projection onto the plane xy.

Functions α_1 and α_2 may define a one dimensional curve Γ as:

$$\Gamma:\ \{\mathbf{q} \in \mathbb{R}^3 | \{\alpha_1(\mathbf{q}) = 0\} \cap \{\alpha_2(\mathbf{q}) = 0\}\} \tag{3}$$

Notice that, since $\{\alpha_1 = 0\}$ is cylindric and every point of $\{\alpha_2 = 0\}$ has a unique projection onto the xy plane, the curve Γ is closed, continuous, and also has a unique projection onto the plane xy. Figure 1 presents an example that illustrates the composition of a curve from functions α_1 and α_2.

The problem that we are addressing in this paper is to make the set of robots Ω converge to and circulate along Γ. This may be written as:

Problem statement. Given the curve Γ as defined in (3), design a controller $\dot{\mathbf{q}}_i = \mathbf{u}_i$ for every robot $\omega_i \in \Omega$ that: (i) guides $\mathbf{q}_i$ from its initial condition $\mathbf{q}_i(0) \in \mathbb{R}^3$ to Γ and (ii) once in Γ enforces $\mathbf{q}_i$ to traverse this curve in

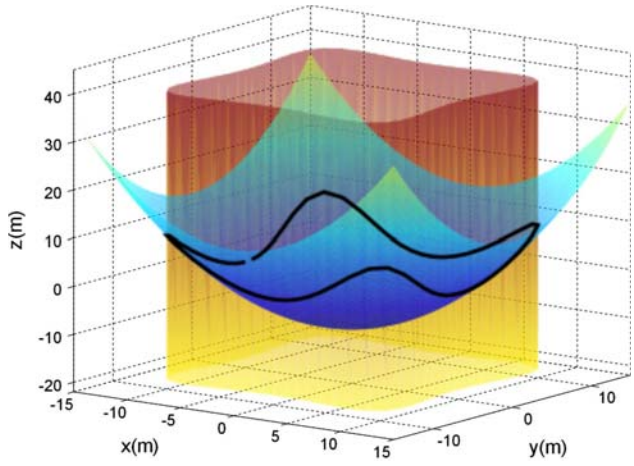

Figure 1. Two manifolds $\{\alpha_1 = 0\}$ and $\{\alpha_2 = 0\}$ with their intersection curve Γ.

a fixed direction, while avoiding collisions with other robots, that is:

$$\|\mathbf{q}_i(t) - \mathbf{q}_j(t)\| - (r_i + r_j) > 0 \quad \forall t \geq 0,$$
$$\forall(\omega_i, \omega_j) \in [\Omega \times \Omega],\ \omega_i \neq \omega_j.$$

The solution to the stated problem is presented in the next section.

3. Methodology

To solve the problem stated in the previous section, we propose the use of individual control inputs of the form:

$$\mathbf{u}_i = -\varphi_i f_{\alpha_2}(\nabla(\alpha_1^2)) - \lambda_i f_{\alpha_1}(\nabla(\alpha_2^2)) + \rho_i \nabla\alpha_1 \times \nabla\alpha_2, \quad (4)$$

where $\nabla(\alpha_k^2)$ stands for the gradient of the square of α_k, and function $f_{\alpha_k}(\mathbf{b}) : \mathbb{R}^3 \mapsto \mathbb{R}^3$ is defined by

$$f_{\alpha_k}(\mathbf{b}) = \begin{cases} \mathbf{b} & \text{if } [\nabla(\alpha_k^2)]^T\mathbf{b} \geq 0 \\ \pi(\mathbf{b}, \mathcal{N}([\nabla(\alpha_k^2)]^T)) & \text{otherwise} \end{cases}.$$

The operator $\pi(\mathbf{b}, \mathcal{N}([\nabla(\alpha_k^2)]^T))$ gives the orthogonal projection of $\mathbf{b}$ onto the null space of $[\nabla(\alpha_k^2)]^T$. The *modulating functions* ρ_i, φ_i, and λ_i, that will be shortly defined, are of the form:

$$\rho_i(\mathbf{q}_i, \mathbf{q}_{\Theta_i}) : \mathbb{R}^{3(M+1)} \mapsto [0, 1],$$

$$\varphi_i(\mathbf{q}_i, \mathbf{q}_{\Theta_i}) : \mathbb{R}^{3(M+1)} \mapsto [0, 1],$$

$$\lambda_i(\mathbf{q}_i, \mathbf{q}_{\Theta_i}) : \mathbb{R}^{3(M+1)} \mapsto [0, 1],$$

where $\mathbf{q}_{\Theta_i}$ is a vector such that its elements are the sphere centers $\mathbf{q}_j$'s of the corresponding robots $\omega_j \in \Theta_i$, and M is the cardinality of the detection set Θ_i defined as:

Definition 1. The detection *set of a robot ω_i is composed by all robots in Ω that are inside its spheric sensing range parametrized by R_i*:

$$\Theta_i \stackrel{\Delta}{=} \{\omega_j \in \Omega \,|\, \{\Delta_{ij} \leq R_i\},\ j \neq i\},$$

where

$$\Delta_{ij} \stackrel{\Delta}{=} \|\mathbf{q}_i - \mathbf{q}_j\|.$$

The intuition behind the definition of the vector field in (4) is as follows. The first two terms are responsible for the convergence of the robots' configuration to Γ. The first term defines a vector that, mostly, points towards the level set $\alpha_1(\mathbf{q_i}) = 0$ while the vector defined by the second term points towards $\alpha_2(\mathbf{q}) = 0$. When these two vectors are competitive, i.e. one term has a component in the opposite direction of the other, function $f_{\alpha_k}(\mathbf{b})$ removes this component by projecting one vector in the null space of the other. The third component of (4) is orthogonal to the other two, thus tangent to the level sets of α_1 and α_2. This tangential component ensures circulation of the robots along the curve. Functions φ_i, λ_i, and ρ_i are in place to modulate the three components of each individual control law in order to prevent inter-robot collisions. A collision avoidance approach is required to assign proper values to these functions. We will now provide several useful definitions prior to detailing this approach.

Definition 2. *For all robots $\omega_i \in \Omega$*, the augmented radius, $\tilde{r}$, *is defined as $\tilde{r} \stackrel{\Delta}{=} r_i + \tau_i$ such that τ_i is positive and is greater than the maximum r_i among all robots in Ω. Notice that the augmented radius is unique for all robots in Ω.*

The augmented radius is important in our approach as it creates a region around the robots that, in deadlock conditions, may be occupied by other robots. This will become clear in the next section.

Definition 3. *The* collision distance δ_{ij} *between a pair is given by:*

$$\delta_{ij} \triangleq \begin{cases} \frac{\Delta_{ij}^2-(2\tilde{r}+\epsilon)^2}{R_i^2-(2\tilde{r}+\epsilon)^2} & \text{if } \Delta_{ij} \geq 2\tilde{r}+\epsilon \\ 0 & \text{otherwise} \end{cases},$$

where ϵ *is a positive constant*.

Definition 4. *The* emergency stop function *induced by a pair* $(\omega_i, \omega_j) \in [\Omega \times \Omega]$ *is given by*:

$$\delta_{ij}^* \triangleq \begin{cases} 1 & \text{if } \Delta_{ij} > (2\tilde{r}+\epsilon) \\ \frac{\Delta_{ij}^2-(2\tilde{r})^2}{(2\tilde{r}+\epsilon)^2-(2\tilde{r})^2} & \text{if } 0 \leq \Delta_{ij}-2\tilde{r} \leq \epsilon \\ 0 & \text{otherwise} \end{cases}.$$

Definition 5. *The* tangential priority Λ_{ij} *function between a pair of robots is given by*:

$$\Lambda_{ij} = \Lambda_{\mathbf{q}_i\mathbf{q}_j} \triangleq (\mathbf{q}_i - \mathbf{q}_j)^T [\nabla\alpha_1(\mathbf{q}_i) \times \nabla\alpha_2(\mathbf{q}_i)],$$

Definition 6. *The* priority sets *related to each component of the vector field are given by*:

$$\Xi_\varphi^i : \{\omega_j \in \Theta_i \,|\, |\alpha_1(\mathbf{q}_i)| > |\alpha_1(\mathbf{q}_j)|\},$$

$$\Xi_\lambda^i : \{\omega_j \in \Theta_i \,|\, |\alpha_2(\mathbf{q}_i)| > |\alpha_2(\mathbf{q}_j)|\},$$

$$\Xi_\rho^i : \{\omega_j \in \Theta_i \,|\, \Lambda_{ij} < \Lambda_{ji}\}.$$

Figure 2 presents an example of the priority sets in Definition 6. Still, related to this definition, it must be noticed that conditions $\{|\alpha_1(\mathbf{q}_i)| = |\alpha_1(\mathbf{q}_j)|\}$, $\{|\alpha_2(\mathbf{q}_i)| = |\alpha_2(\mathbf{q}_j)|\}$ and $\{\Lambda_{ji} = \Lambda_{ij}\}$ are not relevant for practical applications since they occur only when the pair of robots are located on zero-measure regions of $\mathbb{R}^3$. Thus, we can conclude that each priority set is pairwise-selective, that is:

$$\omega_j \in \Xi^i \Leftrightarrow \omega_i \notin \Xi^j.$$

Therefore, these sets provide a strong pairwise priority in the sense that one element of the pair will always have priority over the other element, with no ambiguities. With the aid of the previous definitions, we define the following functions:

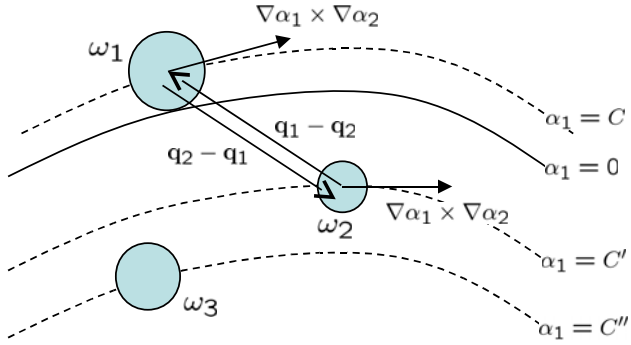

Figure 2. Example of definition 6. Three robots are positioned such that $\alpha_1(\mathbf{q}_1) = C$, $\alpha_1(\mathbf{q}_2) = C'$, $\alpha_1(\mathbf{q}_3) = C''$, where $C<C'<C''$. Therefore, assuming that all robots are detectable by the others, $\Xi_\varphi^1 = \{\}$, $\Xi_\varphi^2 = \{\omega_1\}$, and $\Xi_\varphi^3 = \{\omega_1, \omega_2\}$, indicating that no other robot has priority in relation to ω_1 in the $\nabla(\alpha_1^2)$ component of the field, and only ω_1 has priority in relation to ω_2. Regarding the tangential priority, assuming that the black arrows represent $\nabla\alpha_1(\mathbf{q}_i) \times \nabla\alpha_2(\mathbf{q}_i)$, it can be noticed that $\Xi_\rho^1 = \{\omega_2\}$ while $\Xi_\rho^2 = \{\}$. By inspection, $\Xi_\rho^3 = \{\omega_1, \omega_2\}$.

$$\xi_l^i(\Theta_i) = \begin{cases} \prod\limits_{\omega_j \in \Xi_l^i} |\delta_{ij}| & \text{if } \Xi_l^i \neq \varnothing \\ 1 & \text{otherwise} \end{cases},$$

$$\theta_l^i(\Theta_i) = \begin{cases} \prod\limits_{\omega_j \in \Theta_i} |\delta_{ij}^*| & \text{if } \Theta_i \neq \varnothing \\ 1 & \text{otherwise} \end{cases},$$

where l is equal to φ, λ, or ρ. Then, the values of the functions φ_i, λ_i and ρ_i are set as:

$$\varphi_i = \xi_\varphi^i \theta_\varphi^i, \quad \lambda_i = \xi_\lambda^i \theta_\lambda^i, \quad \rho_i = \xi_\rho^i. \tag{5}$$

From the above definitions, one can conclude that functions φ_i, λ_i and ρ_i modulates each component of the vector field (4) in function of the robots' proximity and priority. It can be observed that if a robot ω_j has priority over robot ω_i in a given component, that is, ω_j is in the Ξ^i relative to this component, and the collision distance δ_{ij} between the two robots is approximately null (it must be noted that δ_{ij} is defined using the augmented radius plus ϵ), the function associated with the component will be equal to zero at ω_i, while ω_j will be allowed to move at the direction of this component. Thus, the collision avoidance scheme establishes a strong priority between any pair of robots in Ω in the three components of the control law (4). A robot will stop at a given component when the distance between a pair reaches a critical value and this robot has no priority in that component, thus allowing the other robot to move. If a pair of robots

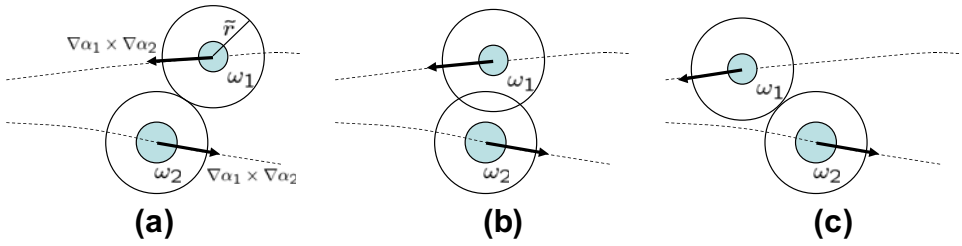

Figure 3. Example of Assumption 3. (a) The robots are at distance $2\tilde{r}$ in $t = t_1$; (b) For all $t > t_1$ and $t < T$ robot ω_1 can move by following $\nabla\alpha_1 \times \nabla\alpha_2$, while ω_2 remains still, given that $\Xi_\rho^2 = \{\omega_1\}$; (c) At time T the distance between the robots is greater than $2\tilde{r}$. In these figures, the dashed lines represent the integral curves of $\nabla\alpha_1 \times \nabla\alpha_2$.

reaches the distance given by $2\tilde{r}$, both robots will stop at the two gradient components, as ensured by δ_{ij}^*, allowing the robots to move only in the tangential direction to escape from the deadlock, provided that Assumption 3, related to the geometry of the curve, is valid, as will be discussed in next section. An example of such a situation is shown in Figure 3, that also illustrates the necessity of the augmented radius definition.

It is important to emphasize that φ_i, λ_i, and ρ_i are continuous functions since functions ξ_l^i and θ_l^i are continuous.

4. Analysis

It is essential to show that the closed-loop system provides convergence to Γ. This section presents two lemmas and a theorem that demonstrates the effectiveness of our approach. To prove the first lemma, two assumptions are made:

Assumption 1. *The robots' initial conditions are inside a bounded region* $\mathcal{B} \subset \mathbb{R}^3$ *such that* $C_1 < \alpha_1(\mathbf{q}) < C_2$ and $D_1 < \alpha_2(\mathbf{q}) < D_2$, *where* $C_1 < 0$, $D_1 < 0$, $C_2 > 0$, $D_2 > 0$ *and*: (i) $\Delta_{ij} > 2\tilde{r} + \epsilon\, \forall \omega_i, \forall \omega_j \in \Omega$, *where* ϵ *is a positive value*, (ii) $\nabla\alpha_1(\mathbf{q_i}) \neq \mathbf{0}\, \forall \omega_i \in \Omega$.

This assumption guarantees that the robots start in a bounded region of the workspace, as required by our proofs. Moreover, it also guarantees that there is no collision among the robots in the initial condition and that all robots do not start at the critical points of α_1.

Assumption 2. *The set* $\nabla\alpha_1(\mathbf{q}) = \mathbf{0}$, *which depends on the nature of the curve, is repulsive*, i.e. *the vector field in the neighborhood of the set repels the robot from the set. Also*, $\nabla\alpha_1(\mathbf{q}) \cap \Gamma = \varnothing$.

Assumption 2 is in place to guarantee that the robots will not be attracted by a local minimum of α_1. Thus, we are assuming that all critical points of α_1 are saddle, unstable points. A proper choice of α_1 may assure this property, as shown in [2].

Definition 7. *A condition* $g = 0$ *is* nonpersistent over time *if* $g = 0$ *at a finite time* T *and there exists a finite time* $T' > T$ *such that* $g \neq 0$.

Lemma 1. *A robot* $\omega_i \in \Omega$, *following the vector field given by (4) asymptotically converges to* Γ *and, once in the curve, circulates along the curve in a fixed direction if the conditions* $\varphi_i = 0$, $\lambda_i = 0$, *and* $\rho_i = 0$ *are nonpersistent over time*.

Proof. Consider the Lyapunov-candidate function $V(\alpha_1, \alpha_2) = (\alpha_1)^2 + (\alpha_2)^2$, which is clearly positive-semidefinite. Also, the set $\mathcal{B}_L = \{\mathbf{q}_i \in \mathbb{R}^3 | V(\alpha_1(\mathbf{q}_i), \alpha_2(\mathbf{q}_i)) < L\}$ is bounded for $0 < L < \infty$. For robot ω_i, the time derivative of V is given by:

$$\begin{aligned}\frac{dV(\alpha_1(\mathbf{q}_i(t)), \alpha_2(\mathbf{q}_i(t)))}{dt} &= \nabla V^T \dot{\mathbf{q}}_i \\ &= -\nabla V^T(\varphi_i f_{\alpha_2}(\nabla(\alpha_1^2)) \\ &\quad + \lambda_i f_{\alpha_1}(\nabla(\alpha_2^2)) - \rho_i \nabla\alpha_1 \times \nabla\alpha_2) \\ &= -2(\alpha_1\nabla\alpha_1 + \alpha_2\nabla\alpha_2)^T(\varphi_i f_{\alpha_2}(\nabla(\alpha_1^2)) \\ &\quad + \lambda_i f_{\alpha_1}(\nabla(\alpha_2^2)) - \rho_i \nabla\alpha_1 \times \nabla\alpha_2) \\ &= -2(\alpha_1\nabla\alpha_1 + \alpha_2\nabla\alpha_2)^T(\varphi_i f_{\alpha_2}(\nabla(\alpha_1^2)) \\ &\quad + \lambda_i f_{\alpha_1}(\nabla(\alpha_2^2))).\end{aligned}$$

Since the vector $(\varphi_i f_{\alpha_2}(\nabla(\alpha_1^2)) + \lambda_i f_{\alpha_1}(\nabla(\alpha_2^2)))$ has nonnegative projection onto $\alpha_1\nabla\alpha_1$ and $\alpha_2\nabla\alpha_2$, and φ_i and λ_i are nonnegative, it follows that

$$\frac{dV(\alpha_1(\mathbf{q}_i(t)), \alpha_2(\mathbf{q}_i(t)))}{dt} \leqslant 0\ \forall t \geqslant 0,\ \forall \omega_i \in \Omega.$$

As shown in Lemma 4 (Appendix A), the time derivative of V is null only when $\varphi_i\alpha_1 = 0$ and $\lambda_i\alpha_2 = 0$.

This guarantees asymptotic convergence to Γ, provided that φ_i and λ_i are not always null. Therefore, in the limit, as time goes to infinity, the time derivative of V goes to zero and the robot configuration $\mathbf{q}_i(t)$ converges to Γ, where $\alpha_1 = 0$ and $\alpha_2 = 0$. We also have that

$$\lim_{\mathbf{q}_i \to \Gamma} \varphi_i f_{\alpha_2}(\nabla(\alpha_1^2(\mathbf{q}_i))) = \mathbf{0},$$

$$\lim_{\mathbf{q}_i \to \Gamma} \lambda_i f_{\alpha_1}(\nabla(\alpha_2^2(\mathbf{q}_i))) = \mathbf{0},$$

which means that only the tangential component $\rho_i \nabla\alpha_1 \times \nabla\alpha_2$ of the vector field (4) remains as the robot approaches the curve. As is proved in Lemma 3 (Appendix A), $\nabla\alpha_1$ and $\nabla\alpha_2$ are linearly independent and are never null at Γ. Thus, it is guaranteed that, $\rho_i \nabla\alpha_1 \times \nabla\alpha_2$ is null only if ρ_i is null. If this is a nonpersistent situation, circulation is guaranteed. □

The previous lemma shows that a robot converges and circulates Γ if the conditions $\varphi_i = 0$, $\lambda_i = 0$, and $\rho_i = 0$ are nonpersistent. It is still necessary to guarantee this situation for all robots in Ω. We start with an assumption.

Assumption 3. *For every pair of configurations* $\mathbf{q}_1 \in \mathcal{B}$ *and* $\mathbf{q}_2 \in \mathcal{B}$ *such that* $\|\mathbf{q}_1 - \mathbf{q}_2\| = 2\tilde{r}$ *and* $\Lambda_{\mathbf{q}_1\mathbf{q}_2} > \Lambda_{\mathbf{q}_2\mathbf{q}_1}$, *there exists a time* T *such that the integral curve* $\kappa(t)$ *of the vector field* $\mathbf{k} = \nabla\alpha_1 \times \nabla\alpha_2$ *that passes through the point* $\mathbf{q}_1$ *at time* $t_1 < T$ *satisfies the following properties:* (i) $\| \kappa(t) - \mathbf{q}_2 \| > r_i + r_j$, *for* $t_1 < t < T$, (ii) $\| \kappa(T) - \mathbf{q}_2 \| > 2\tilde{r} + \epsilon$, *where* ϵ *is a positive value, and* (iii) $\Lambda_{\kappa(t)\mathbf{q}_2} > \Lambda_{\mathbf{q}_2\kappa(t)}$.

This assumption is a strong one. For a pair of robots, it guarantees that once both gradient components of the field are set to zero (a situation that happens when $\|\mathbf{q}_1 - \mathbf{q}_2\| = 2\tilde{r}$), one of the robots may still have space to move in the tangential direction $\nabla\alpha_1 \times \nabla\alpha_2$. In Figure 3, for example, because robot ω_1 has priority over robot ω_2, robot ω_2 stops while ω_1 is able to escape by following the tangential component of the vector field. If Assumption 3 was not satisfied, robot ω_1 would get too close to ω_2, thus causing a collision. In this case, the distance between the integral curves of $\nabla\alpha_1 \times \nabla\alpha_2$ (dashed lines in Figure 3) would be smaller than $r_1 + r_2$. By properly tuning C_1 and C_2 in Assumption 1, one can avoid part of this problem, which is caused by the intersection of smaller level-sets of α_1 and α_2. However, depending on the curvature and the torsion of the integral curves of $\nabla\alpha_1 \times \nabla\alpha_2$, and also on the robots' radii, this issue may appear in other regions of the workspace, thus justifying Assumption 3. It is important to note that this assumption is common to most multi-robot strategies that consider generic curves and nonpoint robots, such as [18]. Unfortunately, there is still no published work that deals with the design of a curve that respects this assumption. On the other hand, it is not too difficult to find curves that satisfy Assumption 3 for a given set $\mathcal{B}$.

Before we continue, we define the scalar function $W : \mathbb{R}^{3N} \to \mathbb{R}^+$ as

$$W(\mathbf{x}) = \sum_{i=1}^{N} V(\mathbf{q}_i), \tag{6}$$

where $\mathbf{x} = [\mathbf{q}_1^T \dots \mathbf{q}_N^T]^T$ and $V(\mathbf{q}_i) = \alpha_1^2(\mathbf{q}_i) + \alpha_2^2(\mathbf{q}_i)$.

Lemma 2. *There exists a finite number of robots* N_{max} *such that*:

(i) *if there is a robot* $\omega_i \in \Omega$, $\mathbf{q}_i \notin \Gamma$ and $\nabla\alpha_1(\mathbf{q}_i(t)) \neq 0 \, \forall t \geq 0$, then the condition

$$\frac{dW(\mathbf{x})}{dt} = 0$$

is nonpersistent over time.

(ii) *if* $\nabla\alpha_1(\mathbf{q}_i(t)) \neq 0 \, \forall t \geq 0$, *and* $\mathbf{q}_i \in \Gamma \ \forall i$ *then the condition*

$$\sum_{i=1}^{N} \| \dot{\mathbf{q}}_i \| = 0$$

is also nonpersistent over time.

Proof. Let the number of robots N be equal to two. According to Lemma 4 $\frac{dV(\mathbf{q}_i(t_0))}{dt} = 0$ if and only if $\varphi_i(t_0)\alpha_1(\mathbf{q}_i) = \lambda_i(t_0)\alpha_2(\mathbf{q}_i) = 0$. Therefore, if $\mathbf{q}_i \notin \Gamma$ and $\frac{dV(\mathbf{q}_i(t_0))}{dt} = 0$, then $\varphi_i(t_0) = 0$ or $\lambda_i(t_0) = 0$. Consider the worst case scenario where $\| \mathbf{q}_i - \mathbf{q}_j \| = \tilde{r}_i + \tilde{r}_j$. In this case $\delta_{ij}^* = 0$, which implies that only the tangential component direction is available for motion. According to Assumption 3 and the proposed control law, at $t = T'$ we will have $\| \mathbf{q}_i - \mathbf{q}_j \| > \tilde{r}_i + \tilde{r}_j + \epsilon$. If one robot is at the curve and the other is not, then $\frac{dW(\mathbf{x})}{dt} \neq 0$ at $t = T'$ since $\delta_{ij} \neq 0$ and $\delta_{ij}^* \neq 0$. If both robots are at the curve, then $\sum_{i=1}^{N} \| \dot{\mathbf{q}}_i(t) \| \neq 0$ since there is at least one robot moving in the tangential direction. If both robots are out of the curve then at $t = T'$, at least one robot with priority in one of the convergence directions will move and consequently $\frac{dW(\mathbf{x})}{dt} \neq 0$.

Since the desired curve is closed, there exists a finite number of robots M such that $\| \mathbf{q}_i - \mathbf{q}_j \| < \tilde{r}_i + \tilde{r}_j$, $\forall i, j$ if all the robots are placed at the desired curve. In this case, the robots will never move and $\sum_{i=1}^{N} \| \dot{\mathbf{q}}_i \| = 0 \ \forall t$. Now, suppose these M robots are at the desired curve and one robot ω_i is out of the curve. Consider also a configuration such that $\| \mathbf{q}_i - \mathbf{q}_j \| = \tilde{r}_i + \tilde{r}_j$, $\Lambda_{ij} < \Lambda_{ji}$,

where ω_j is a robot at the desired curve. In this case, the robots will never move, as ω_j will not be able to move due to the presence of the other robots at Γ and $\frac{dW(\mathbf{x})}{dt} = 0 \ \forall t$. Therefore, it follows that there exists N_{max} in the interval $[2, M+1]$ that guarantees the nonpersistence of conditions (i) and (ii). □

Although an exact value for $N_{\max}$ is hard to obtain, given that it depends on the geometric properties of α_1, α_2, and on the size of the robots, we have not experienced problems with the choice of this number. In practical applications of boundary coverage, we always have success if all robots in the team can fit on the curve, considering their augmented radius. Thus, by combining Lemmas 1 and 2 and assuming $N < N_{\max}$, we are able to state the following theorem, which guarantees the effectiveness of the proposed vector field.

Theorem 1. *Each robot ω_i in the group of robots Ω following the vector field given by (4) asymptotically converges to Γ and, once on the curve, circulates along the curve in a fixed direction. Furthermore, no collisions will occur between any pairs of robots*.

Proof. By Lemma 2 it is possible to see that $\frac{dV(\mathbf{q}_i(t_0))}{dt} = 0$ is nonpersitent over time for all robots, unless all robots are on the curve. Therefore, it is possible to infer that $\varphi_i = 0$ and $\lambda_i = 0$ will be nonpersistent over time for robots that are not on the curve. Hence, by Lemma 1, all robots will converge to the curve as time tends to infinity. Similarly, since $\sum_{i=1}^{N} \| \dot{\mathbf{q}}_i \| = 0$ is nonpersistent, ρ_i cannot be zero for all robots simultaneously, consequently guaranteeing circulation along the curve via Lemma 1. Finally, due to the properties of the collision avoidance approach (5) and Assumption 3, the robots will never collide and for every pair of robots we will have $\| \mathbf{q}_i - \mathbf{q}_j \| \geqslant r_i + r_j, \forall t$. □

5. Experimental results

In this section, we focus on the development of an approach capable of enabling a single quadrotor robot to control given the kinematic inputs defined in Section 3 and evaluate the decentralized control laws proposed in this work on a team of quadrotors. To this end, we first develop the dynamic model and propose onboard feedback control for attitude stabilization and position control in $SE(3)$ following the methods proposed in [19,20] and detail how we generate kinematic inputs given this dynamic model and onboard feedback control. We then discuss the implementation and infrastructure details followed by experiment design. Finally, we review the experimental evaluation of these methods on teams of up to six quadrotors.

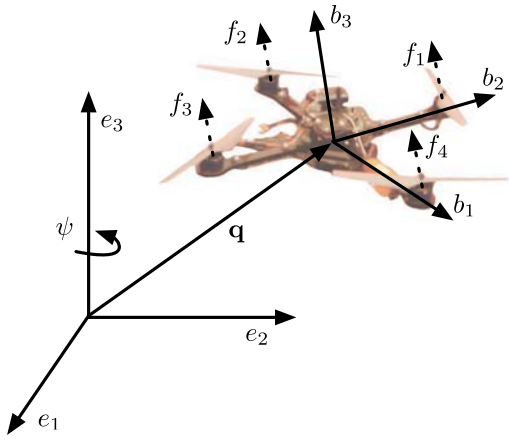

Figure 4. The vehicle model. The position and orientation of the robot in the global frame are denoted by $\mathbf{q}$ and $\mathbf{R}$, respectively. Control inputs (7) consider both position, $\mathbf{q}$, and the orientation, ψ, of the vehicle about the global z-axis (e_3). Each propeller generates a thrust f_i along the body-fixed z-axis (b_3).

5.1. Modeling and control

Consider the quadrotor robot model shown in Figure 4 with mass m and rotational inertia $\mathbf{J} \in \mathbb{R}^{3\times3}$. Define the position and rotation of the vehicle in the inertial frame as $\mathbf{q} \in \mathbb{R}^3$ and $\mathbf{R} \in SO(3)$, respectively. The angular velocity of the vehicle, $\mathbf{\Omega} \in \mathbb{R}^3$, is defined as

$$\dot{\mathbf{R}} = \mathbf{R}\hat{\mathbf{\Omega}},$$

where the hat operator $\hat{\cdot}: \mathbb{R}^3 \to SO(3)$ is defined such that $\hat{x}y = x \times y$ for all $x, y \in \mathbb{R}^3$.[19] Given that the ith propeller generates the thrust output f_i as a function of propeller rotational speed, the dynamic model of the vehicle follows:

$$m\ddot{\mathbf{q}} = f\mathbf{R}\mathbf{e}_3 - mg\mathbf{e}_3$$

$$\mathbf{J}\dot{\mathbf{\Omega}} + \mathbf{\Omega} \times \mathbf{J}\mathbf{\Omega} = \mathbf{M},$$

with $\mathbf{e}_3 = [0,\ 0,\ 1]^{\mathrm{T}}$, $\mathbf{M} = [M_1,\ M_2,\ M_3]^{\mathrm{T}}$, and

$$\begin{bmatrix} f \\ M_1 \\ M_2 \\ M_3 \end{bmatrix} = \begin{bmatrix} 1 & 1 & 1 & 1 \\ d & 0 & -d & 0 \\ 0 & d & 0 & -d \\ -c & c & -c & c \end{bmatrix} \begin{bmatrix} f_1 \\ f_2 \\ f_3 \\ f_4 \end{bmatrix},$$

where d is the distance from the robot center of mass to the rotor and c is an aerodynamic drag term that relates differences in propeller speed to yawing moment about the body z-axis.

Due to the design of the system actuation, it is well known that the quadrotor is underactuated and differentially flat.[21] The four system inputs allow us to specify the force along the body-fixed z-axis (b_3) and the three moments in the body-fixed frame. We accordingly choose four output variables and define the desired state of the robot as:

$$\mathbf{x}_{\mathrm{d}} = \begin{bmatrix} \mathbf{q}_{\mathrm{d}} \\ \psi_{\mathrm{d}} \end{bmatrix} = \begin{bmatrix} x_{\mathrm{d}} \\ y_{\mathrm{d}} \\ z_{\mathrm{d}} \\ \psi_{\mathrm{d}} \end{bmatrix}, \tag{7}$$

where ψ_{d} is the desired vehicle yaw (rotation about the inertial z-axis). In this work, we restrict ψ to be constant and zero (e.g. $\psi_{\mathrm{d}} = 0$). Given the kinematic control, $\mathbf{u}$, we transform the desired vehicle commands to the desired state

$$\begin{aligned} \mathbf{x}_{\mathrm{d},t} &= \begin{bmatrix} \mathbf{q}_{t-1} \\ 0 \end{bmatrix} + \begin{bmatrix} \mathbf{u}_t \\ 0 \end{bmatrix} \Delta t \\ \dot{\mathbf{x}}_{\mathrm{d},t} &= \begin{bmatrix} \mathbf{u}_t \\ 0 \end{bmatrix} \\ \ddot{\mathbf{x}}_{\mathrm{d},t} &= \begin{bmatrix} \frac{\mathbf{u}_t - \mathbf{u}_{t-1}}{\Delta t} \\ 0 \end{bmatrix} \end{aligned}. \tag{8}$$

Following the attitude stabilization approach proposed in [19], we design the force and moment inputs, f and M_i, based on the desired input $\mathbf{x}_{\mathrm{d}}$:

$$\begin{aligned} f &= (-k_{\mathbf{q}}\mathbf{e}_{\mathbf{q}} - k_{\dot{\mathbf{q}}}\mathbf{e}_{\dot{\mathbf{q}}} + mg\mathbf{e}_3 + \ddot{\mathbf{q}}_{\mathrm{d}}) \cdot \mathbf{R}\mathbf{e}_3 \\ \mathbf{M} &= -k_{\mathbf{R}}\mathbf{e}_{\mathbf{R}} - k_{\Omega}\mathbf{e}_{\Omega} + \boldsymbol{\Omega} \times \mathbf{J}\boldsymbol{\Omega} \end{aligned} \tag{9}$$

with the error terms defined as follows:

$$\mathbf{e}_{\mathbf{q}} = \mathbf{q} - \mathbf{q}_{\mathrm{d}}$$

$$\mathbf{e}_{\dot{\mathbf{q}}} = \dot{\mathbf{q}} - \dot{\mathbf{q}}_{\mathrm{d}}$$

$$\mathbf{e}_{\mathbf{R}} = \frac{1}{2\sqrt{1 + \mathrm{tr}[\mathbf{R}_d^{\mathrm{T}}\mathbf{R}]}} \left(\mathbf{R}_{\mathrm{d}}^{\mathrm{T}}\mathbf{R} - \mathbf{R}^{\mathrm{T}}\mathbf{R}_{\mathrm{d}}\right)^{\vee}$$

$$\mathbf{e}_{\Omega} = \boldsymbol{\Omega} - \mathbf{R}^{\mathrm{T}}\mathbf{R}_{\mathrm{d}}\boldsymbol{\Omega}_{\mathrm{d}}$$

and dropping any dependence on time for clarity of presentation. The operator $(\cdot)^{\vee}$ is the inverse of the hat operator $\hat{\cdot}$ and, therefore, it is a mapping from $SO(3)$ to $\mathbb{R}^3$. The gains $k_{\mathbf{r}}$, $k_{\dot{\mathbf{r}}}$, k_R, and k_{Ω} are selected to ensure stable performance. See [19,20] for further explanation of the derivation of these error terms and proofs of stability and convergence of the control system to the desired inputs.

The above attitude stabilization approach operates in $SO(3)$ (as compared to the traditional Euler-angle parameterization approach [22]) and benefits from a stability basin of attraction that includes the full space of rotation matrices (excluding an exact inversion). Note that we assume

$$\| -k_{\mathbf{q}}\mathbf{e}_{\mathbf{q}} - k_{\dot{\mathbf{q}}}\mathbf{e}_{\dot{\mathbf{q}}} + mg\mathbf{e}_3 + \ddot{\mathbf{q}}_{\mathrm{d}} \| > 0$$

given the magnitude of the gains and the fact that we do not anticipate accelerations approaching $1g$ and thus define $\mathbf{R}_{\mathrm{d}}$ with respect to ψ_{d} such that $\mathbf{R}_{\mathrm{d}} = [\mathbf{r}_1,\ \mathbf{r}_2,\ \mathbf{r}_3]$ and

$$\mathbf{r}_1 = \mathbf{r}_2 \times \mathbf{r}_3$$

$$\mathbf{r}_2 = \frac{\mathbf{r}_3 \times [\cos\psi_{\mathrm{d}},\ \sin\psi_{\mathrm{d}},\ 0]}{\| \mathbf{r}_3 \times [\cos\psi_{\mathrm{d}},\ \sin\psi_{\mathrm{d}},\ 0] \|}$$

$$\mathbf{r}_3 = \frac{-k_{\mathbf{q}}\mathbf{e}_{\mathbf{q}} - k_{\dot{\mathbf{q}}}\mathbf{e}_{\dot{\mathbf{q}}} + mg\mathbf{e}_3 + \ddot{\mathbf{q}}_{\mathrm{d}}}{\| -k_{\mathbf{q}}\mathbf{e}_{\mathbf{q}} - k_{\dot{\mathbf{q}}}\mathbf{e}_{\dot{\mathbf{q}}} + mg\mathbf{e}_3 + \ddot{\mathbf{q}}_{\mathrm{d}} \|}.$$

Additionally, the moment stabilization proposed in [19] includes higher order inertial cancelation terms that we neglect because their effects are insignificant in the experiments for this work.

5.2. Implementation details

The robots used in this work are sold commercially [23] and follow a standard four-propeller design (Figure 5). The pose of the quadrotor is observed using a Vicon motion capture system at 150 Hz.[24] The pose is numerically differentiated to compute the linear and angular velocities of the robot. These values are available to Matlab via ROS [25] and a ROS-Matlab bridge.[26] All control inputs are computed at 50 Hz in Matlab using the

Figure 5. The team of six quadrotors used in experimentation.

latest state estimate at the rate of the Vicon. This computation emulates decentralized control by computing each robot's control in Matlab independent of global knowledge except for the positions of neighbor vehicles. The commands in Matlab are bridged to ROS where they are interpreted by a finite-state machine (FSM) which aids in the experimental process.[22] The FSM manages the individual robots, places the robots at the appropriate initial conditions, then relinquishes control to Matlab where the inputs (7) are computed from (8). Throughout the experiments, we saturate the commanded velocity of the robots such that

$$\bar{\mathbf{u}}_i = v_{\max}\frac{\mathbf{u}_i}{\| \mathbf{u}_i \|}$$

where $v_{\max} = 0.2$ m/s and send $\bar{\mathbf{u}}_i$ to each vehicle. The FSM computes the required inputs (Section 5.1) specified by the Matlab commands and transmits these values to the robot via Zigbee at a fixed rate of 50 Hz. This fixed rate is due to the limited bandwidth of Zigbee (57.6 kbps). These commands are interpreted by the attitude and body-fixed thrust controllers (9) operating on each robot's programmable embedded microprocessor and applied at a 1 kHz update rate.

Figure 7. The team of six quadrotors during an experimental trial tracking the desired curve while avoiding inter-robot collisions.

5.3. Results

We conducted a series of trials that considered a curve Γ defined by the intersection of a cylindric surface and a slightly modified paraboloid specified by

$$\alpha_1 = ax^4 - bx^2y^2 + cy^4 - 1,$$

$$\alpha_2 = z - d(y^2 + x^2) + e,$$

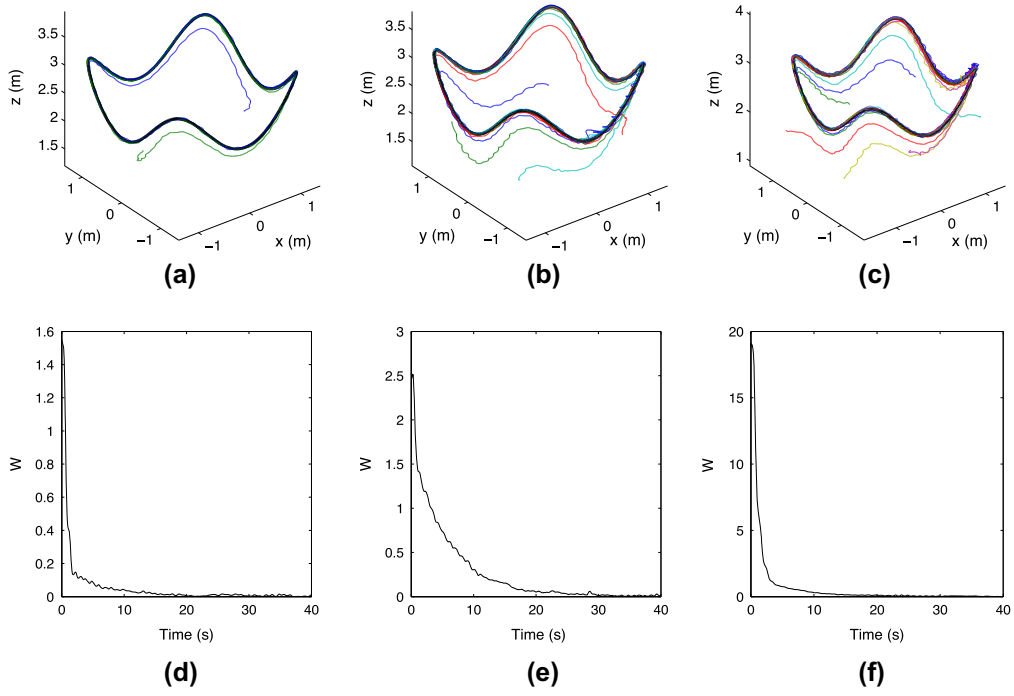

Figure 6. Two, four, and six robots control to the desired curve using proposed vector field (left, middle, and right columns, respectively). The paths followed by each of the robots to the desired curve (shown in black) are depicted in (a)–(c). Despite the increasing number of robots, in (d)–(f) we see that, since W in (6) goes to 0 as the time increases, the robots converge to the desired curve.

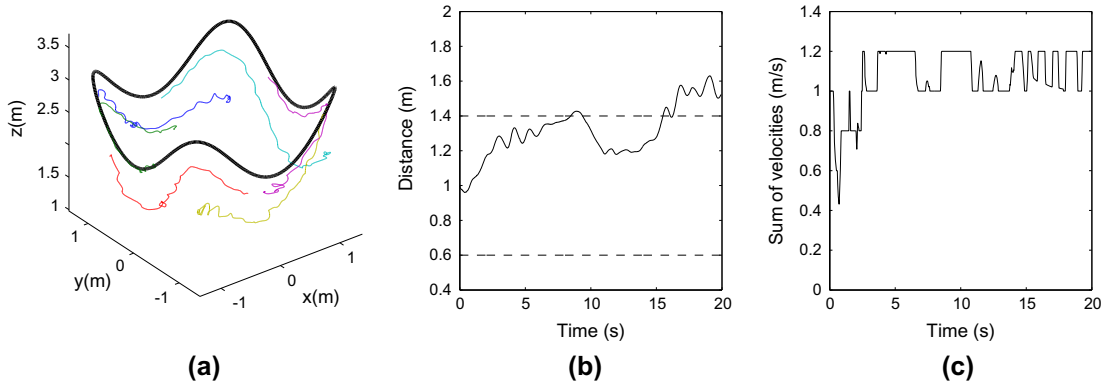

Figure 8. To study the impact of the kinematic assumption on the performance of the dynamic team of robots, we start the robots in close proximity and increase the sensing distance of each robot. We see in (a) that robots experience degraded tracking performance resulting from the prioritization approach. However, from (b), which shows the distance between the pair of robots with the smallest pairwise distance, it is clear that robots successfully enforce the required inter-robot distance. The application of collision-avoidance is best seen by investigating the magnitude of the sum of the robot velocities (c), where the expected velocity without collision avoidance is the product of the number of robots and saturation velocity (in this case it is 1.2 m/s).

with $a = 0.3$, $b = 0.03$, $c = 0.3$, $d = -0.5$, and $e = 1.0$. The two manifolds $\{\alpha_1 = 0\}$ and $\{\alpha_2 = 0\}$ with their intersection Γ are similar to the ones shown in Figure 1. In these examples, the robots are identical with radius $r_i = 0.3$ m, augmented radius $\tilde{r} = 0.6$ m, and sensing radius $R_i = 1.0$ m.

In Figure 6, we consider the convergence of teams of two, four, and six robots to the same curve. Figures 6 (a)–(c) show the robots' paths for these situations while Figures 6(d)–(f) show the behavior of function W, indicating the convergence of the team to the curve. Figure 7 shows a snapshot of one of the experiments. Videos of these experiments can be found at http://www.cpdee.ufmg.br/ coro/movies/curvecontrol.

In Section 5.1, we provide the modeling and control of the quadrotor robot to enable the application of proposed vector field on the experimental platforms. As seen in the previous results, this approach enables the robots to converge to the curve. However, we observe that the cost of the kinematic assumption becomes more pronounced as the number and frequency of collision avoidance maneuvers becomes more frequent. For this reason, we include an additional study that aims to illustrate this point and motivate future research.

Clearly from Figure 8, we see a degradation in control performance for a team of six robots with an increase in the sensing radius (now $R_i = 1.4$ m). We begin the experiment by ensuring that several of the robots are within the sensing radius of the others, thus requiring the robots to enforce inter-robot collision avoidance. Indeed, one of the greatest sources of decreased control performance is presumption of a kinematic agent in the prioritization methodology. While we see that the robots continue to control such that inter-robot distances increase, the immediate and frequent change in commanded velocity results in poor overall performance. As such, the extension of these methods to dynamic systems is clearly motivated and a focus of future research.

6. Conclusions and future work

This paper presented a decentralized method for multi-robot control that guarantees convergence and circulation of a group of aerial robots along closed, simple, and static curves defined in three-dimensional spaces. The method is based on an individual vector field that attracts the robots to a curve and on a collision avoidance scheme that modulates the components of the field. This scheme relies only on neighboring information obtained by local sensors or limited range communication devices. Experimental results with a team of quadrotors indicate that the method may be used to solve real world problems.

This work focused on groups of unmanned holonomic rotorcrafts that admits null and negative velocities. Therefore, the proposed approach is not applicable to aerial robots with minimal forward speed and bounded turning radius constraints. Our future work includes the design of controllers to these kind of robot. The methodology also assumes a kinematic robot. Although this may be a practical assumption in several situations, our experimental results show that it will be important to consider the robots' dynamics in our future developments.

It is also important to say that our approach is provably correct as long as some assumptions are verified. A current limitation is the fact that there is no

analytical method to verify some of these conditions. Also, there is still no algorithm to build a curve in 3D that satisfies all assumptions. This will be also considered a future direction of research. In spite of this limitation, in all the simulations and experiments we have run, we have not observed any convergence problem or collisions among robots.

Acknowledgments

This work is part of the CNPq/NSF cooperation program, Grant no. 49.0743/2006-4. It is partially supported by FAPEMIG (Brazil), CNPq (Brazil), CAPES (Brazil), FINEP (Brazil), NSF Grant IIS-0,427,313, ARO Grant W911NF-05-1-0219, ONR Grants N00014-07-1-0829 and N00014-08-1-0696, and ARL Grant W911NF-08-2-0004. G.A.S. Pereira holds a scholarship from CNPq.

Notes on contributors

Luciano C.A. Pimenta received the B.S., M.Sc., and Ph.D. degrees in electrical engineering from the Universidade Federal de Minas Gerais (UFMG), Belo Horizonte, Brazil, in 2003, 2005, and 2009, respectively. From April 2007 to June 2008, he was a visiting Ph.D. student at the General Robotics, Automation, Sensing and Perception (GRASP) Laboratory at the University of Pennsylvania, Philadelphia, USA. He is currently an Assistant Professor with the Department of Electronic Engineering at UFMG. His research interests include robotics, multi-robot systems, and control theory.

Guilherme A.S. Pereira received the B.S. and M.S. degrees in electrical engineering and the Ph.D. degree in computer science from the Federal University of Minas Gerais (UFMG), Belo Horizonte, Brazil, in 1998, 2000, and 2003, respectively. He received the Gold Medal Award from the Engineering School of UFMG for garnering first place among the electrical engineering students in 1998. He was, from November 2000 to May 2003, a Visiting Scientist at the General Robotics, Automation, Sensing and Perception (GRASP) Laboratory, University of Pennsylvania, Philadelphia. Since July 2004, he is an Assistant Professor of the Electrical Engineering Department at the Federal University of Minas Gerais (DEE/UFMG), where he is the director of the Computer Systems and Robotics (CORO) Laboratory, one of the laboratories that compose the Group for Research and Development of Autonomous Vehicles (PDVA) at UFMG. His research interests include cooperative robotics, robot navigation, autonomous vehicles development, computer vision, and distributed sensing. Dr. Pereira is a Member of IEEE and Sociedade Brasileira de Automática (SBA).

Mateus Mariano Gonçalves was born in 1983 in Belo Horizonte, Minas Gerais, Brazil. He has a B.S. in Control Engineering (2008) and a M.S. in Electrical Engineering (2010) by the Federal University of Minas Gerais, where he worked with the decentralized motion planning of aerial robots swarms using potential fields. Currently, he is a First Lieutenant of Brazilian Navy Corps of Engineers, taking part in the research that will lead to the construction of the first Brazilian nuclear-propelled submarine.

Nathan Michael is an assistant research professor in the Robotics Institute at Carnegie Mellon University. Prior to this appointment, he was a Research Assistant Professor in the Department of Mechanical Engineering at the University of Pennsylvania. He received a Ph.D. from the Department of Mechanical Engineering at the University of Pennsylvania in 2008 and transitioned into a position in the Research Faculty in 2010. His research interests include the topics of estimation and control for ground and aerial robots with extensions to multi-robot systems.

Matthew Turpin is a Ph.D. candidate in the Department of Mechanical Engineering and Applied Mechanics at the University of Pennsylvania. He works on concurrent assignment and planning of trajectories as well as formation control for MAVs.

Vijay Kumar is the UPS Foundation Professor in the School of Engineering and Applied Science at the University of Pennsylvania, and on sabbatical leave at White House Office of Science and Technology Policy where he serves as the assistant director for robotics and cyber physical systems. He received his Bachelors of Technology from the Indian Institute of Technology, Kanpur and his Ph.D. from The Ohio State University in 1987. He has been on the Faculty in the Department of Mechanical Engineering and Applied Mechanics with a secondary appointment in the Department of Computer and Information Science at the University of Pennsylvania since 1987. He served as the Deputy Dean for Research in the School of Engineering and Applied Science from 2000 to 2004. He directed the GRASP Laboratory, a multidisciplinary robotics and perception laboratory, from 1998 to 2004. He was the Chairman of the Department of Mechanical Engineering and Applied Mechanics from 2005 to 2008. He then served as the Deputy Dean for Education in the School of Engineering and Applied Science from 2008 to 2012. He is a Fellow of the American Society of Mechanical Engineers (ASME) and the Institution of Electrical and Electronic Engineers (IEEE). He

has served on the editorial boards of the IEEE Transactions on Robotics and Automation, IEEE Transactions on Automation Science and Engineering, ASME Journal of Mechanical Design, the ASME Journal of Mechanisms and Robotics and the Springer Tract in Advanced Robotics (STAR). He is the recipient of the 1991 National Science Foundation Presidential Young Investigator award, the 1996 Lindback Award for Distinguished Teaching (University of Pennsylvania), the 1997 Freudenstein Award for significant accomplishments in mechanisms and robotics, the 2012 ASME Mechanisms and Robotics Award, the 2012 IEEE Robotics and Automation Society Distinguished Service Award and a 2012 World Technology Network Award. He has won best paper awards at DARS 2002, ICRA 2004, ICRA 2011, and RSS 2011 and has advised doctoral students who have won Best Student Paper Awards at ICRA 2008, RSS 2009, and DARS 2010. He is also a Distinguished Lecturer in the IEEE Robotics and Automation Society and an elected member of the Robotics and Automation Society Administrative Committee (2007–2012). His research interests are in robotics, specifically multi-robot systems, and micro aerial vehicles.

References

[1] Sabattini L, Cristian S, Fantuzzi C. Closed-curve path tracking for decentralized systems of multiple mobile robots. J. Intell. Robot. Syst. 2012. doi: 10.1007/s10846-012-9763-9.

[2] Gonçalves VM, Pimenta LCA, Maia CA, Dutra BCO, Pereira GAS. Vector fields for robot navigation along time-varying curves in n-dimensions. IEEE Trans. Robot. 2010;26:647–659.

[3] Iscold P, Pereira GAS, Torres LAB. The development of a hand-launched small UAV for ground reconnaissance. IEEE Transactions on Aerospace and Electronic Systems 2010;46:335–348.

[4] Ceccarelli N, Marco MD, Giannitrapani A. Collective circular motion of multi-vehicle systems. Automatica 2008;44: 3025–3035.

[5] Lawrence DA, Frew EW, Pisano WJ. Lyapunov vector fields for autonomous unmanned aircraft flight control. J. Guid. Control Dyn. 2009;31(5):1220–1229.

[6] Zhang F, Leonard NE. Coordinated patterns of unit speed particles on a closed curve. Syst. Control Lett. 2007;56:397–407.

[7] Pimenta LCA, Mendes ML, Mesquita RC, Pereira GAS. Fluids in electrostatic fields: an analogy for multi-robot control. IEEE Trans. Magn. 2007;43:1765–1768.

[8] Hsieh MA, Kumar V, Chaimowicz L. Decentralized controllers for shape generation. Robotica. 2008;26:691–701.

[9] Hernandez S, Paley DA. Stabilization of collective motion in a time-invariant flowfield on a rotating sphere. Proc. Am. Control Conf. 2009:623–628

[10] Frew EW, Lawrence DA, Dixon C, Elston J, Pisano WJ. Lyapunov guidance vector fields for unmanned aircraft applications. Proc. Am. Control Conf. 2007:371–376.

[11] Alonso-Mora J, Breitenmoser A, Rufli M, Siegwart R, Beardsley P. Multi-robot system for artistic pattern formation. Proc. of the IEEE Int. Conf. on Robot. Autom. 2011:4512–4517.

[12] Sugihara K, Suzuki I. Distributed algorihtms for formation of geometric patterns with many mobile robots. Journal of Robotic Systems 1996;13(3):127–139.

[13] Bennet DJ, McInnes CR. Verifiable control of a swarm of unmanned aerial vehicles. J. Proc. Inst. Mech. Eng, Part G: J. Aerosp. Eng. 2009;223:939–953.

[14] Paul T, Krogstad TR, Gravdahl JT. Modelling of UAV formation flight using 3D potential field. Simul. Model. Pract. Theory. 2008;16:1453–1462.

[15] Nelson DR, Blake D, McLain TW, Beard RW. Vector field path following for small unmanned air vehicles. Proc. Am. Control Conf. 2006:5788–5794.

[16] Gan SK, Sukkarieh S. Multi-UAV target search using explicit decentralized gradient-based negotiation. Proc. IEEE Int. Conf. Robot. Autom. 2011:751–756.

[17] Esposito JM, Kumar V. A method for modifying closed-loop motion plans to satisfy unpredictable dynamic constraints at runtime. Proc. IEEE Int. Conf. Robot. Autom. 2002:1691–1696.

[18] Hsieh MA, Loizou S, Kumar V. Stabilization of multiple robots on stable orbits via local sensing. Proc. IEEE Int. Conf. Robot. Autom. 2007:2312–2317.

[19] Lee T, Leok M, McClamroch NH. Geometric tracking control of a quadrotor UAV on SE(3). In: Proc. IEEE Conf. Decision and Control; 2010; Atlanta, GA. p. 5420–5425.

[20] Lee T. Geometric Tracking Control of the Attitude Dynamics of a Rigid Body on SO(3). In: Proc. Am. Control Conf.; 2011; San Francisco, CA. p. 1200–1205.

[21] Van Nieuwstadt MJ, Murray RM. Real-time trajectory generation for differentially flat systems. International Journal of Robust and Nonlinear Control 1998;8 (11):995–1020.

[22] Michael N, Mellinger D, Lindsey Q, Kumar V. The GRASP multiple micro UAV testbed. IEEE Robotics and Automation Magazine 2010;17(3):56–65.

[23] Ascending Technologies, GmbH, accessed August 16, 2012. Available from: http://www.asctec.de

[24] Vicon Motion Systems, Inc., accessed August 16, 2012. Available from: http://www.vicon.com.

[25] Robot Operating System (ROS), accessed August 16, 2012. Available from: http://www.ros.org

[26] ROS-Matlab Bridge, accessed August 16, 2012. Available from: http://www.github.com/nmichael/ipc-bridge

Appendix. Additional Lemmas

Lemma 3. *Vectors* $\nabla\alpha_1(\mathbf{q})$ *and* $\nabla\alpha_2(\mathbf{q})$ *are linearly independent for every* $\mathbf{q} \in \mathbb{R}^3$ *where* $\nabla\alpha_1(\mathbf{q}) \neq \mathbf{0}$. *Also, if* $\nabla\alpha_1(\mathbf{q}) \neq \mathbf{0}$ *then* $\alpha_1(\mathbf{q})\nabla\alpha_1(\mathbf{q}) + \alpha_2(\mathbf{q})\nabla\alpha_2(\mathbf{q}) \neq \mathbf{0}$ *for every point* $\mathbf{q} \notin \Gamma$.

Proof. By Equation (2) we have

$$\frac{\partial}{\partial z}\alpha_2(x,y,z) = \frac{\partial}{\partial z}[\sigma z - \Phi(x,y)] = \sigma,\ \sigma \neq 0.$$

Then, it is impossible to have $\nabla\alpha_2(\mathbf{q}) = \mathbf{0}, \forall \mathbf{q} \in \mathbb{R}^3$. As α_1 is cylindric and depends only on x and y, we also have that

$$\frac{\partial}{\partial z}\alpha_1(x,y,z) = 0,$$

implying that $\nabla\alpha_1(\mathbf{q})$ and $\nabla\alpha_2(\mathbf{q})$ are linearly independent, since the z-axis component of $\nabla\alpha_1$ is identically null at every point in $\mathbb{R}^3$, the same z-axis component of $\nabla\alpha_2$ is non-null for all points in $\mathbb{R}^3$ and $\nabla\alpha_1(\mathbf{q}) \neq \mathbf{0}$ by hypothesis.

Also, it can be noted that $\mathbf{q} \notin \Gamma \Longleftrightarrow \{\mathbf{q} \in \mathbb{R}^3 | \{\alpha_1(\mathbf{q}) \neq \mathbf{0}\} \cup \{\alpha_2(\mathbf{q}) \neq \mathbf{0}\}\}$. Therefore, for $\mathbf{q} \notin \Gamma$:

$$\alpha_1(\mathbf{q})\nabla\alpha_1(\mathbf{q}) + \alpha_2(\mathbf{q})\nabla\alpha_2(\mathbf{q}) \neq \mathbf{0}.$$

□

Lemma 4. *Let* $\omega_i \in \Omega$ *and* $V(\mathbf{q})$ *be defined as in Lemma 1. If* $\mathbf{q}_i \notin \Gamma$ *and* $\nabla\alpha_1(\mathbf{q}_i) \neq \mathbf{0}$ *at time* T, *then*

$$\left.\frac{dV(\alpha_1(\mathbf{q}_i(t)), \alpha_2(\mathbf{q}_i(t)))}{dt}\right|_{t=T} \triangleq \left.\frac{dV(\mathbf{q}_i(t))}{dt}\right|_{t=T} = 0$$

if and only if $\varphi_i(T)\alpha_1(\mathbf{q}_i) = \lambda_i(T)\alpha_2(\mathbf{q}_i) = 0$.

Proof. As presented in the proof of Lemma 1,

$$\frac{dV(\alpha_1(\mathbf{q}_i(t)), \alpha_2(\mathbf{q}_i(t)))}{dt} = -2(\alpha_1\nabla\alpha_1 + \alpha_2\nabla\alpha_2)^T\mathbf{a}$$

where $\mathbf{a} = \varphi_i f_{\alpha_2}(\nabla(\alpha_1^2)) + \lambda_i f_{\alpha_1}(\nabla(\alpha_2^2))$. According to Lemma 3, if $\nabla\alpha_1(\mathbf{q}) \neq \mathbf{0}$ then $\alpha_1(\mathbf{q})\nabla\alpha_1(\mathbf{q}) + \alpha_2(\mathbf{q})\nabla\alpha_2(\mathbf{q}) \neq \mathbf{0}$ for every point $\mathbf{q} \notin \Gamma$. Moreover, $(\alpha_1\nabla\alpha_1)^T\mathbf{a} \geq 0$ and $(\alpha_2\nabla\alpha_2)^T\mathbf{a} \geq 0$. As $(\alpha_1\nabla\alpha_1)^T\mathbf{a} = 0$ and $(\alpha_2\nabla\alpha_2)^T\mathbf{a} = 0$ if and only if $\varphi_i(T)\alpha_1(\mathbf{q}_i) = \lambda_i(T)\alpha_2(\mathbf{q}_i) = 0$, then the Lemma is proved. □